

เพปไทด์นิวคลีอิกแอซิดโพรบที่ว่องไวทางเคมีไฟฟ้า



นางสาวจุฑาทิพย์ คงเพชร



วิทยานิพนธ์นี้เป็นส่วนหนึ่งของการศึกษาตามหลักสูตรปริญญาวิทยาศาสตรมหาบัณฑิต
สาขาวิชาเคมี ภาควิชาเคมี
คณะวิทยาศาสตร์ จุฬาลงกรณ์มหาวิทยาลัย
ปีการศึกษา 2556
ลิขสิทธิ์ของจุฬาลงกรณ์มหาวิทยาลัย



5471934623

ELECTROCHEMICALLY ACTIVE PEPTIDE NUCLEIC ACID PROBES

Miss Jutatip Kongpeth



A Thesis Submitted in Partial Fulfillment of the Requirements
for the Degree of Master of Science Program in Chemistry

Department of Chemistry

Faculty of Science


Chulalongkorn University

Academic Year 2013

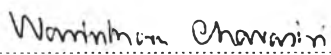
Copyright of Chulalongkorn University

Thesis Title ELECTROCHEMICALLY ACTIVE PEPTIDE NUCLEIC
ACID PROBES
By Miss Jutatip Kongpeth
Field of Study Chemistry
Thesis Advisor Professor Tirayut Vilaivan, D.Phil.

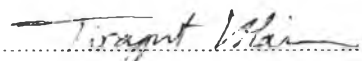
Accepted by the Faculty of Science, Chulalongkorn University in Partial
Fulfillment of the Requirements for the Master's Degree

.....Dean of the Faculty of Science
(Professor Supot Hannongbua, Dr.rer.nat.)

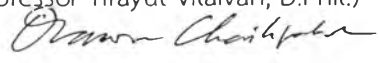
THESIS COMMITTEE

.....Chairman

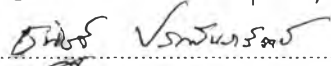
(Assistant Professor Warinthorn Chavasiri, Ph.D.)

.....Thesis Advisor

(Professor Tirayut Vilaivan, D.Phil.)

.....Examiner

(Professor Orawon Chailapakul, Ph.D.)

.....Examiner

(Thanit Praneenarat, Ph.D.)

.....External Examiner

(Chaturong Suparpprom, Ph.D.)



จุฑาทิพย์ คงเพชร : เพปไทด์นิวคลีอิกแอซิดโพรบที่ว่องไวทางเคมีไฟฟ้า.
(ELECTROCHEMICALLY ACTIVE PEPTIDE NUCLEIC ACID PROBES) อ.ที่ปรึกษา
วิทยานิพนธ์หลัก: ศ. ดร. อธิรุท วิไลวัลย์, 108 หน้า.

ตัวตรวจวัดดีเอ็นเอถูกนำมาใช้งานอย่างแพร่หลายทั้งในงานด้านการวินิจฉัยทาง
การแพทย์ การตรวจสอบคุณภาพสิ่งแวดล้อม การควบคุมคุณภาพอาหาร และงานด้านนิติ
วิทยาศาสตร์ โดยทั่วไปตัวตรวจวัดลำดับเบสบนดีเอ็นเอประกอบด้วยโมเลกุลตรวจจับหรือที่
เรียกว่า “โพรบ” ซึ่งสามารถจับกับดีเอ็นเอเป้าหมายได้อย่างจำเพาะเจาะจง การจับกันระหว่างโพร
บและโมเลกุลเป้าหมายก่อให้เกิดสัญญาณที่ตรวจวัดได้โดยผ่านกลไกการแปลงสัญญาณที่
เหมาะสม โดยตัวตรวจวัดดีเอ็นเอที่ดีควรตรวจวัดได้อย่างรวดเร็ว แม่นยำ ใช้สารตัวอย่างใน
ปริมาณที่น้อย พกพาสะดวก ปลอดภัย และราคาถูก ซึ่งสิ่งเหล่านี้เป็นไปได้โดยอาศัยเทคนิคทาง
เคมีไฟฟ้า เพปไทด์นิวคลีอิกแอซิดหรือพีเอ็นเอเป็นสารเลียนแบบดีเอ็นเอที่นิยมใช้เป็นตัวตรวจจับ
ในการตรวจวัดดีเอ็นเอ เนื่องจากมีความสามารถในการจับยึดและมีความเลือกจำเพาะสูงกับดีเอ็น
เอได้ดีกว่าดีเอ็นเอธรรมชาติหรือสารเลียนแบบดีเอ็นเอชนิดอื่นๆ เพื่อเป็นการผนวกจุดเด่นของพี
เอ็นเอและเคมีไฟฟ้า ในงานวิจัยนี้ จึงสนใจพัฒนาการตรวจวัดลำดับเบสบนดีเอ็นเอโดยใช้พีโรลิดิ
นิลเพปไทด์นิวคลีอิกแอซิด (acpcPNA) เป็นตัวตรวจวัด ผ่านเทคนิคทางเคมีไฟฟ้าโดยไม่มีการตรึง
โพรบลงบนขั้วไฟฟ้า ผู้วิจัยได้สังเคราะห์สารที่ว่องไวทางเคมีไฟฟ้าหลายชนิด เช่น แอนทราควิโนน
และ เมทิลีนบลู แล้วติดฉลากลงบนพีโรลิดินิลพีเอ็นเอผ่านปฏิกิริยาเอซิลเลชัน (acylation)
จากนั้นจึงทำให้บริสุทธิ์ด้วยเทคนิค reverse phase HPLC และพิสูจน์เอกลักษณ์ด้วยเทคนิค
MALDI-TOF MS พีเอ็นเอที่ติดฉลากสามารถจับยึดกับดีเอ็นเอเป้าหมายได้อย่างแข็งแรงและ
จำเพาะเจาะจงโดย UV melting experiment ต่อมาจึงได้ศึกษาการตรวจวัดสัญญาณทาง
เคมีไฟฟ้าบน screen-printed carbon electrode (SPCE) ซึ่งเป็นขั้วไฟฟ้าที่มีราคาถูกด้วย
เทคนิค square-wave voltammetry (SWV) แรงกระทำระหว่างประจุไฟฟ้าของ acpcPNA
หรือโมเลกุลลูกผสม acpcPNA-DNA กับพื้นผิวของอิเล็กโทรดจะควบคุมการถ่ายโอนอิเล็กตรอน
ระหว่างพีเอ็นเอโพรบและอิเล็กโทรด ซึ่งเป็นรากฐานของกลไกการเปลี่ยนแปลงสัญญาณ พีเอ็นเอ
ที่ติดฉลากด้วยแอนทราควิโนนบนอิเล็กโทรดที่ดัดแปลงด้วยพอลิเมอร์ PQDMAEMA ที่ม
ีความจำเพาะเจาะจงสูง โดยมีค่า LOD และ LOQ อยู่ในระดับนาโนโมลาร์ และได้แสดงการ
ตรวจวัดลำดับเบสบนดีเอ็นเอในสารตัวอย่างจริงที่เพิ่มปริมาณด้วยเทคนิค LAMP และ PCR ได้
นอกจากนี้ยังศึกษาผลของประจุบนพื้นผิวของอิเล็กโทรดและพีเอ็นเอ เพื่อทำความเข้าใจถึงกลไก
การแปลงสัญญาณอีกด้วย ดังนั้นการตรวจวัดทางเคมีไฟฟ้าที่มีศักยภาพสูงระบบใหม่แบบไม่มีการ
ตรึงโพรบ โดยอาศัยพีโรลิดินิลพีเอ็นเอโพรบที่ว่องไวทางเคมีไฟฟ้าร่วมกับขั้วไฟฟ้าแบบ SPCE ถูก
พัฒนาจนเป็นผลสำเร็จ

ภาควิชา เคมี

สาขาวิชา เคมี

ปีการศึกษา 2556

ลายมือชื่อนิสิต จุฑาทิพย์ คงเพชร

ลายมือชื่อ อ.ที่ปรึกษาวิทยานิพนธ์หลัก

5471934623 : MAJOR CHEMISTRY

KEYWORDS: ACPCPNA / DNA DETECTION / ELECTROCHEMICAL DETECTION / SCREEN PRINTED ELECTRODE

JUTATIP KONGPETH: ELECTROCHEMICALLY ACTIVE PEPTIDE NUCLEIC ACID PROBES.

ADVISOR: PROF. TIRAYUT VILAIVAN, D.Phil., 108 pp.

DNA sensors are useful in various applications including medical diagnosis, environmental monitoring, food quality control, and forensic science. The sensor usually consists of a sensing element known as a "probe" that can bind specifically with the DNA target. The binding between the probe and the target creates a measurable signal via an appropriate signal transduction mechanism. Ideal DNA sensors should allow rapid detection, provide high specificity and sensitivity, require small sample volumes and require low cost instrumentation. Electrochemical DNA sensors are one type of DNA sensors that meet all the above requirements. Peptide nucleic acid or PNA is a unique DNA analogue that is often employed as the sensing element in DNA sensors due to its superior affinity and specificity in recognition of DNA than natural DNA or other DNA analogues. To combine the advantages of PNA and electrochemistry in DNA sensing, an electrochemical DNA sensor based on pyrrolidinyl peptide nucleic acid (acpcPNA) probe that does not require probe immobilization was developed. Various kinds of redox-active redox reporters including anthraquinone and methylene blue were synthesized and introduced onto acpcPNA via acylation chemistry. The redox-active acpcPNAs were purified by reverse phase HPLC and characterized by MALDI-TOF MS. The labeled acpcPNA formed hybrids to DNA with high thermal stability and specificity according to UV melting experiments. The immobilization-free electrochemical DNA detection platform was next developed on an inexpensive screen-printed carbon electrode (SPCE) by using a square-wave voltammetric (SWV) technique. Electrostatic interactions between the acpcPNA probe, the acpcPNA-DNA hybrid and the electrode surface modulate the electron transfer between the labeled acpcPNA probe and the electrode, providing the basis of the signal transduction. As an example, a highly specific signal-on detection of DNA by SWV with LOD and LOQ in the low nanomolar range was achieved using anthraquinone-labeled acpcPNA probes on PQDMAEMA-modified SPCE electrodes. Applications of the technique for analysis of real DNA samples that had been amplified by LAMP or PCR were demonstrated. Furthermore, the effects of the charges on the surface of the electrode and on the acpcPNA probe were studied to obtain further insights into the mechanism of the signal transduction. Accordingly, a novel and highly promising immobilization-free electrochemical DNA sensor based on redox-active acpcPNA probe on SPCE was successfully developed.

Department: Chemistry

Field of Study: Chemistry

Academic Year: 2013

Student's Signature

Jutatip Kongpeth

Advisor's Signature

Tirayut Vilaivan



2189366678

ACKNOWLEDGEMENTS

I here by would like to express my sincere appreciation to my thesis advisor Professor Dr. Tirayut Vilaivan for good guidance and well encouragement throughout my Master's degree education and research at Chulalongkorn University.

Furthermore, I would also like to thank my thesis committee Assistant Professor Dr. Warinthorn Chavasiri, Professor Dr. Orawon Chailapakul, Dr. Thanit Praneenarat and Dr. Chaturong Suparpprom for their valuable comments and suggestions.

I would like to thank Organic Synthesis Research Unit (OSRU), Electrochemistry and Optical Spectroscopy Research Unit and Center of Innovative Nanotechnology (CIN) for glassware, chemicals and instrumentations and I also would like to thank Thailand Research Fund (RTA5280002, DPG5780002) and Teaching Assistant Scholarship, Chulalongkorn University for all financial supports.

In addition, I also gratefully acknowledge Associate Professor Dr. Voravee Hoven and Miss Pornpen Sae-ung for kindly providing the PQDMAEMA and PAC samples; Assistant Professor Dr. Piyasak Chaumpluk, Department of Botany, Faculty of Science, Chulalongkorn University for kind support of the WSSV samples; Mr. Sakda Jampasa, Program in Petrochemical and Polymer Science, Faculty of Science, Chulalongkorn University for his kind support of HPV samples and help with electrochemical concepts and experiments; Prof. Dr. Nattiya Hirankarn, Department of Microbiology, Faculty of Medicine, Chulalongkorn University for her kind support of HLA samples.

Special thanks are also extended to all members of TV group for their kindness and helpful advices; Mr. Poomrat Rattanarat and Mr. Eakkasit Punrat for their helpful comments and suggestions to improve my research.

Finally, I would like to especially thank my family for their love, inspiration and support throughout my life.



2189366578

CONTENTS

	Page
THAI ABSTRACT	iv
ENGLISH ABSTRACT	v
ACKNOWLEDGEMENTS	vi
CONTENTS	vii
LIST OF TABLES	x
LIST OF FIGURES.....	xi
LIST OF SCHEMES.....	xviii
LIST OF ABBREVIATIONS AND SYMBOLS.....	xix
CHAPTER I INTRODUCTION.....	1
1.1 Introduction	1
1.2 Objectives of the research.....	3
1.3 Scope of the research.....	3
CHAPTER II THOERY AND LITERATURE REVIEWS	4
2.1 Deoxyribonucleic acid (DNA)	4
2.2 Peptide nucleic acid (PNA).....	4
2.3 Electrochemical DNA biosensors employing immobilized DNA or PNA probes... 6	
2.4 Immobilization-free electrochemical DNA biosensors	10
CHAPTER III EXPERIMENT	14
3.1 Chemicals and apparatus.....	14
3.2 General procedures.....	16
3.2.1 Synthesis and characterization of electrochemically-active reporters..... 16	
3.2.2 Synthesis of labeled acpcPNA probes..... 18	
3.2.2.1 Synthesis of acpcPNA probes..... 18	
3.2.2.2 Labeling electrochemically-active reporter onto acpcPNA via acylation reaction..... 18	
3.2.2.3 Purification and characterization of labeled acpcPNA probes..... 20	
3.2.2.4 Determination of PNA concentration	20



	Page
3.2.2.5 PNA-DNA binding properties.....	20
3.2.3 Preparation of samples and buffers.....	21
3.2.3.1 Preparation of stock buffer solution used in study of buffer effect	21
3.2.3.2 DNA amplification by Loop-Mediated Isothermal Amplification (LAMP).....	22
3.2.3.3 DNA amplification by PCR.....	23
3.2.3.4 Denaturation of duplex DNA (dsDNA) samples before electrochemical measurement	24
3.2.4 Preparation of electrodes and electrochemical measurements.....	24
3.2.4.1 Preparation of screen printed carbon electrode (SPCE).....	24
3.2.4.2 Electrochemical measurements.....	25
CHAPTER IV RESULTS AND DISCUSSION	26
4.1 Synthesis and characterization of electrochemically-active labeled acpcPNA ..	26
4.2 PNA-DNA binding properties.....	27
4.3 Preparation and characterization of screen-printed carbon electrode (SPCE) ...	30
4.3.1 Preparation of the unmodified, positively and negatively charged polymer modified SPCE	30
4.3.2 Performance of the unmodified, positively charged and negatively charged SPCE.....	31
4.4 Characteristic of electrochemical signal of labeled acpcPNA.....	34
4.5 Proof of principle for immobilization-free DNA sequence detection employing labeled acpcPNA	35
4.6 Comparison of performance of terminally and internally-labeled acpcPNA probes.....	37
4.7 Effects of buffer.....	38
4.8 Reusability of the unmodified SPCE	41
4.9 Positively-charged modified SPCE	42
4.10 Effect of type and pH of buffer	47



2189366678

	Page
4.11 Effect of accumulation potential	47
4.12 The effect of amounts of polymer	48
4.13 Optimization of SWV parameters	50
4.14 Effect of analyte composition.....	53
4.15 Calibration curve.....	54
4.16 Selectivity of the PNA probe.....	55
4.17 Effect of non-complementary DNA	56
4.18 Effect of long and double-stranded DNA targets.....	57
4.19 Detection of blind samples.....	61
4.20 Detection of LAMP-amplified DNA samples.....	62
4.21 Specificity test with real DNA samples.....	63
4.22 Sensitivity of LAMP samples.....	63
4.23 Detection of PCR-amplified DNA samples.....	65
4.24 Understanding the interaction of charges on the SPCE and PNA.....	66
CHAPTER V CONCLUSION	69
REFERENCES	71
APPENDIX.....	79
VITA.....	108



2189366678

LIST OF TABLES

	Page
Table 3.1 PNA probe sequences used in this work.....	19
Table 3.2 Primer sequences used in LAMP amplification of WSSV samples	22
Table 3.3 Primer sequence used in PCR amplification [26].....	23
Table 4.1 Retention time, m/z (MALDI-TOF), and yield of redox-active labeled acpcPNA	27
Table 4.2 Melting temperature of labeled acpcPNA	28
Table 4.3 Redox potential and peak width at half height of 2AQ-T2 in various buffers	40
Table 4.4 Characteristics of the three positively-charged polymers used in this study	44
Table 4.5 Optimization of SWV parameters.....	51



LIST OF FIGURES

	Page
Figure 2.1 Structure of deoxyribonucleic acid (DNA).....	4
Figure 2.2 Structure of (a) aegPNA, (b) γ -PNA and (c) diethylene glycol containing γ -PNA.....	5
Figure 2.3 Structure of acpcPNA.....	6
Figure 2.4 General design of DNA biosensors	6
Figure 2.5 Principles of electrochemical DNA detection based on immobilized probes (A) label free (B) redox indicator (C) redox-labeled probe	7
Figure 2.6 (A) DPV of nucleobase A, T, C and G [52] (B) DPV of nucleobase A, T, C and G before and after MB intercalation in the case of (B) complementary and (C) single base mismatch DNA	7
Figure 2.7 Performance of ferrocene and methylene blue labeled probe immobilization after various scans	10
Figure 2.8 DNA detection by using immobilization free method based on (A) negatively charged and (B) positively charged modified electrode	11
Figure 2.9 Application used in immobilization-free electrochemical DNA sensing method employing (A) labeled PNA probe and isothermal circular strand-displacement DNA polymerization (B) labeled DNA beacon and exonuclease II-assisted target recycling (C) same as (B) but with linear labeled DNA probe	12
Figure 3.1 Synthesis of 4-(anthraquinone-1-yloxy)butyric acid (1AQ)	16
Figure 3.2 Synthesis of 4-(anthraquinone-2-yloxy)butyric acid (2AQ)	17
Figure 4.1 The structure of acpcPNA	26
Figure 4.2 The pattern of the Screen Printed Carbon Electrode used in this work	30
Figure 4.3 Cyclic voltammograms of 1 mM $[\text{Fe}(\text{CN})_6]^{3-/4-}$ in 0.5 M KCl (20 μL) and the linear relationship between anodic peak currents and scan rates on (A) unmodified, (B) 1% PQDMAEMA (positively charged) and (C) 5% PAA (negatively charged) modified SPCE.....	33
Figure 4.4 SWV signals of labeled acpcPNA (50 μM , 20 μL) (A) 1AQ-T2 (yellow) 2AQ-T2 (orange) and (B) MB-T2 in 10 mM phosphate buffer (pH 7.4)	34
Figure 4.5 DNA Biosensors based on redox labeled probe immobilization with (A) a classical probe and (B) a hairpin probe	35



Figure 4.6 SWVs of (left) MB-T9-Lys and (right) 2AQ-T9-Lys (50 μ M, 20 μ L) before and after hybridized with complementary DNA in 10 mM phosphate buffer pH 7.4	36
Figure 4.7 The selectivity of labeled PNA probe (50 μ M, 20 μ L) (A) MB-T9-Lys (terminal) (B) 2AQ-T9-Lys (terminal) (C) T5-MB-T4-Lys (internal) (D) T5-2AQ-T4-Lys (internal) on unmodified SPCE in 10 mM phosphate buffer (pH7.4)	38
Figure 4.8 (Top) SWVs of 2AQ-T2 (50 μ M, 20 μ L) in various buffers and (Bottom) bar graph of the signal received	39
Figure 4.9 Selectivity of 2AQ-PNA (50 μ M, 20 μ L) on unmodified SPCE in various buffers (A) 30 mM acetate buffer (pH 4.6) (B) 10 mM citrate buffer (pH 4.6) (C) 10 mM MES buffer (pH 7.0) (D) 10 mM phosphate buffer (pH 7.4) (E) 10 mM Tris-HCl buffer (pH 8.0) (F) 10 mM Tris-Borate buffer (pH 9.0) ...	41
Figure 4.10 Reusability of the unmodified SPCE. The SWV signal of MB-T9 PNA (50 μ M, 20 μ L) was measured on unmodified, pretreated SPCE in 10 mM phosphate buffer pH 7.4.	42
Figure 4.11 The signal of 2AQ-WSSV-Lys (50 μ M, 20 μ L) in 10 mM phosphate buffer pH 7.0 on the CHT modified SPCE	43
Figure 4.12 Structures of CHT, HTCAA-CHT and PQDMAEMA	44
Figure 4.13 Comparison of the 2AQ-WSSV-Lys (50 μ M, 20 μ L) before and after hybridized with single base mismatched and complementary DNA in 10 mM phosphate buffer (A) pH 5.5, (B) pH 7.4 and (C) pH 8.0 on various positively charged modified SPCE the (left).....	46
Figure 4.14 Effect of buffer to the 2AQ-WSSV-Lys (5 μ M, 20 μ L) signal (left) before and after hybridized with (center) complementary and (right) single base mismatched DNA in 10 mM phosphate buffer pH (purple) 7.0 and (blue) 8.0 and Tris-HCl buffer pH (green) 7.4 and (red) 8.0.....	47
Figure 4.15 Effect of accumulation potential to the signal of hybrid of 2AQ-WSSV-Lys with complementary DNA (5 μ M in 10 mM Tris-HCl buffer pH 8.0, 20 μ L) on 1% PQDMAEMA modified SPCE.	48
Figure 4.16 Effect of the amounts of PQDMAEMA in the modified SPCE to the 2AQ-WSSV-Lys signal ((Top) 500 and (Bottom) 50 nM in 10 mM Tris-HCl Buffer pH 8.0, 20 μ L). The % polymer is expressed as the amount of the polymer (w/v) in the carbon ink mixture used for the electrode screening	50

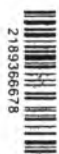


2189366678

	Page
Figure 4.17 Optimization of SWV parameters for the detection of the signal from 2AQ-WSSV-Lys PNA-DNA sample on 0.26% PQDMAEMA modified SPCE (50 nM, 10 mM Tris-HCl buffer pH 8.0, 20 μ L)	52
Figure 4.18 Effect of analyte composition (A) DNA (B) PNA on the 0.26% PQDMAEMA modified SPCE (0.5 μ M in 10 mM Tris-HCl buffer pH 8.0, 20 μ L)	54
Figure 4.19 (Top) Scan of linear range and (Bottom) calibration curve of this system on 0.26% PQDMAEMA modified SPCE in 10 mM Tris-HCl buffer pH 8.0 (20 μ L)	55
Figure 4.20 Selectivity of 2AQ-WSSV-Lys (50 nM, 20 μ L) on 0.26% PQDMAEMA modified SPCE in Tris-HCl buffer at pH 8.0.....	56
Figure 4.21 Effect of non-target DNA (single base mismatched DNA) to the signal of PNA-DNA hybrid (50 nM, 20 μ L) on 0.26% PQDMAEMA modified SPCE in 10 mM Tris-HCl buffer pH 8.0	57
Figure 4.22 Effect of long length target DNA to the signal of PNA-DNA hybrid (50 nM, 20 μ L) on 0.26% PQDMAEMA modified SPCE in 10 mM Tris-HCl buffer pH 8.0	58
Figure 4.23 Invasion of AQ-WSSV-Lys PNA (50 nM) to the 19bp double-stranded DNA targets (50 nM) on 0.26% PQDMAEMA modified SPCE in 10 mM Tris-HCl buffer pH 8.0 (total volume = 20 μ L).....	59
Figure 4.24 Invasion of PNA (50 nM) on the long double strand target DNA (50 nM) in the presence of 100 mM NaCl on 0.26% PQDMAEMA modified SPCE in 10 mM Tris-HCl buffer pH 8.0 (total volume = 20 μ L)	60
Figure 4.25 Invasion of PNA (50 nM) on the long double strand target DNA (50 nM) by using thermal denaturation method on 0.26% PQDMAEMA modified SPCE in 10 mM Tris-HCl buffer at pH 8.0 (total volume = 20 μ L)	60
Figure 4.26 Detection of blind DNA samples using 2AQ-WSSV-Lys probe (50 nM) on the 0.26% PQDMAEMA modified SPCE in 10 mM Tris-HCl buffer pH 8.0 (20 μ L)	61
Figure 4.27 (A) Detection of heat-denatured LAMP WSSV samples at no, 10-fold, 100-fold and 1,000-fold dilution using 2AQ-WSSV-Lys (50 nM) compared with non-template sample and negative control (100 dilution) on 0.26% PQDMAEMA modified SPCE in 10 mM Tris-HCl buffer pH 8.0 (20 μ L) (B) comparison of the signal at various dilution of LAMP samples.....	62



	Page
Figure 4.28 Specificity of 2AQ-WSSV-Lys (50 nM) in detection of heat-denatured LAMP samples on 0.26% PQDMAEMA modified SPCE in 10 mM Tris-HCl buffer pH 8.0 (20 μ L).....	63
Figure 4.29 Sensitivity in detection of heat-denatured LAMP samples at different dilutions (A) 100-fold, (B) 10-fold and (C) no dilution with 2AQ-WSSV-Lys (50 nM) on 0.26% PQDMAEMA modified SPCE in 10 mM Tris-HCl buffer pH 8.0 (20 μ M).....	64
Figure 4.30 Detection of PCR (A) HPV type 16 (HPV-negative C33 was used as negative control sample) and (B) B1502 samples (HLA B1513 was used as negative control sample) on 0.26% PQDMAEMA modified SPCE in 10 mM Tris-HCl buffer pH 8.0 (20 μ L).....	65
Figure 4.31 Comparison of the 2AQ-WSSV-Lys, 2AQ-WSSV-Ser and 2AQ-WSSV-Glu (all at 50 nM) on the (A) positively-charged (B) unmodified (C) negatively-charged modified SPCE in 10 mM Tris-HCl buffer pH 8.0 (20 μ L)	67
Figure 4.32 Comparison of the 2AQ-WSSV-Lys, 2AQ-WSSV-Ser and 2AQ-WSSV-Glu before and after hybridized with complementary DNA on the (A) positively-charged (B) unmodified (C) negatively- charged modified SPCE in 10 mM Tris-HCl buffer pH 8.0 (20 μ L)	68
Figure A1 ^1H NMR spectra of ethyl 4-(anthraquinone-1-oxy)butyrate (400 MHz, CDCl_3) (top) and 4-(anthraquinone-1-oxy)butyric acid (400 MHz, $\text{DMSO}-d_6$) (bottom)	80
Figure A2 ^{13}C NMR spectrum of 4-(anthraquinone-1-oxy)butyric acid (100 MHz, $\text{DMSO}-d_6$)	81
Figure A3 ^1H NMR spectra of ethyl 4-(anthraquinone-2-oxy)butyrate (400 MHz, CDCl_3) (top) and 4-(anthraquinone-2-oxy)butyric acid (400 MHz, $\text{DMSO}-d_6$) (bottom)	82
Figure A4 ^{13}C NMR spectra of ethyl 4-(anthraquinone-2-oxy)butyrate (400 MHz, CDCl_3) (top) and 4-(anthraquinone-2-oxy)butyric acid (400 MHz, $\text{DMSO}-d_6$) (bottom)	83
Figure A5 MALDI-TOF mass spectrum of methylene blue butyric acid (calcd for $[\text{M}+\text{H}]^+ = 357.1$)	84
Figure A6 Determination of molar extinction coefficient (ϵ) of 4-(anthraquinone-1-oxy)butyric acid (top), 4-(anthraquinone-2-oxy)butyric acid (center) and methylene blue butyric acid (bottom)	85



Page

Figure A7 (a) Analytical HPLC chromatogram (ACE 5 C18-AR (150 x 4.6 mm) HPLC column, water(A)/methanol(B) (started with A:B (90:10) for 5 min followed by a linear gradient to A:B (10:90) over a period of 70 min), flow rate 0.5 mL/min) and (b) MALDI-TOF mass spectrum of PNA 1AQ-T2-Lys (calcd for $[M+H]^+$ = 991.3)	86
Figure A8 (a) Analytical HPLC chromatogram (ACE 5 C18-AR (150 x 4.6 mm) HPLC column, water(A)/methanol(B) (started with A:B (90:10) for 5 min followed by a linear gradient to A:B (10:90) over a period of 70 min), flow rate 0.5 mL/min) and (b) MALDI-TOF mass spectrum of PNA 2AQ-T2-Lys (calcd for $[M+H]^+$ = 992.0)	87
Figure A9 (a) Analytical HPLC chromatogram (ACE 5 C18-AR (150 x 4.6 mm) HPLC column, water(A)/methanol(B) (started with A:B (90:10) for 5 min followed by a linear gradient to A:B (10:90) over a period of 70 min), flow rate 0.5 mL/min) and (b) MALDI-TOF mass spectrum of PNA MB-T2-Lys (calcd for $[M+H]^+$ = 1037.4)	88
Figure A10 (a) Analytical HPLC chromatogram (ACE 5 C18-AR (150 x 4.6 mm) HPLC column, water(A)/methanol(B) (started with A:B (90:10) for 5 min followed by a linear gradient to A:B (10:90) over a period of 70 min), flow rate 0.5 mL/min) and (b) MALDI-TOF mass spectrum of PNA 1AQ-T9-Lys (calcd for $[M+H]^+$ = 3429.7)	89
Figure A11 (a) Analytical HPLC chromatogram (ACE 5 C18-AR (150 x 4.6 mm) HPLC column, water(A)/methanol(B) (started with A:B (90:10) for 5 min followed by a linear gradient to A:B (10:90) over a period of 70 min), flow rate 0.5 mL/min) and (b) MALDI-TOF mass spectrum of PNA 2AQ-T9-Lys (calcd for $[M+H]^+$ = 3430.2)	90
Figure A12 (a) Analytical HPLC chromatogram (ACE 5 C18-AR (150 x 4.6 mm) HPLC column, water(A)/methanol(B) (started with A:B (90:10) for 5 min followed by a linear gradient to A:B (10:90) over a period of 70 min), flow rate 0.5 mL/min) and (b) MALDI-TOF mass spectrum of PNA MB-T9-Lys (calcd for $[M+H]^+$ = 3518.0)	91
Figure A13 (a) Analytical HPLC chromatogram (ACE 5 C18-AR (150 x 4.6 mm) HPLC column, water(A)/methanol(B) (started with A:B (90:10) for 5 min followed by a linear gradient to A:B (10:90) over a period of 70 min), flow rate 0.5 mL/min) and (b) MALDI-TOF mass spectrum of PNA T5-1AQ-T4-Lys (calcd for $[M+H]^+$ = 3472.3)	92



	Page
Figure A14 (a) Analytical HPLC chromatogram (ACE 5 C18-AR (150 x 4.6 mm) HPLC column, water(A)/methanol(B) (started with A:B (90:10) for 5 min followed by a linear gradient to A:B (10:90) over a period of 70 min), flow rate 0.5 mL/min) and (b) MALDI-TOF mass spectrum of PNA T5-2AQ-T4-Lys (calcd for $[M+H]^+$ = 3473.9)	93
Figure A15 (a) Analytical HPLC chromatogram (ACE 5 C18-AR (150 x 4.6 mm) HPLC column, water(A)/methanol(B) (started with A:B (90:10) for 5 min followed by a linear gradient to A:B (10:90) over a period of 70 min), flow rate 0.5 mL/min) and (b) MALDI-TOF mass spectrum of PNA T5-MB-T4-Lys (calcd for $[M+H]^+$ = 3473.9)	94
Figure A16 (a) Analytical HPLC chromatogram (ACE 5 C18-AR (150 x 4.6 mm) HPLC column, water(A)/methanol(B) (started with A:B (90:10) for 5 min followed by a linear gradient to A:B (10:90) over a period of 70 min), flow rate 0.5 mL/min) and (b) MALDI-TOF mass spectrum of PNA 2AQ-WSSV-Lys (calcd for $[M+H]^+$ = 4136.7)	95
Figure A17 (a) Analytical HPLC chromatogram (ACE 5 C18-AR (150 x 4.6 mm) HPLC column, water(A)/methanol(B) (started with A:B (90:10) for 5 min followed by a linear gradient to A:B (10:90) over a period of 70 min), flow rate 0.5 mL/min) and (b) MALDI-TOF mass spectrum of PNA 2AQ-WSSV-Ser (calcd for $[M+H]^+$ = 4091.6)	96
Figure A18 (a) Analytical HPLC chromatogram (ACE 5 C18-AR (150 x 4.6 mm) HPLC column, water(A)/methanol(B) (started with A:B (90:10) for 5 min followed by a linear gradient to A:B (10:90) over a period of 70 min), flow rate 0.5 mL/min) and (b) MALDI-TOF mass spectrum of PNA 2AQ-WSSV-Glu (calcd for $[M+H]^+$ = 4132.5)	97
Figure A19 (a) Analytical HPLC chromatogram (ACE 5 C18-AR (150 x 4.6 mm) HPLC column, water(A)/methanol(B) (started with A:B (90:10) for 5 min followed by a linear gradient to A:B (10:90) over a period of 70 min), flow rate 0.5 mL/min) and (b) MALDI-TOF mass spectrum of PNA 2AQ-B1502-Lys (calcd for $[M+H]^+$ = 4351.1)	98
Figure A20 (a) Analytical HPLC chromatogram (ACE 5 C18-AR (150 x 4.6 mm) HPLC column, water(A)/methanol(B) (started with A:B (90:10) for 5 min followed by a linear gradient to A:B (10:90) over a period of 70 min), flow rate 0.5 mL/min) and (b) MALDI-TOF mass spectrum of PNA 2AQ-B1513-Lys (calcd for $[M+H]^+$ = 4414.4)	99



	Page
Figure A21 Melting curves of unmodified PNAs T9-Lys (top) and T4-(apc)-T5-Lys (bottom) (1 μ M) after hybridized with complementary DNA (dA ₉ , 1 μ M, blue) compared with single base mismatched DNA (dA ₅ TA ₄ , 1 μ M, red) in 10 mM phosphate buffer pH 7.0	100
Figure A22 Melting curves of PNAs 1AQ-T9-Lys (top) and T4-1AQ-T5 -Lys (bottom) (1 μ M) after hybridized with complementary DNA (dA ₉ , 1 μ M, blue) compared with single base mismatched DNA (dA ₅ TA ₄ , 1 μ M, red) in 10 mM phosphate buffer pH 7.0.....	101
Figure A23 Melting curves of PNAs 2AQ-T9-Lys (top) and T4-2AQ-T5 -Lys (bottom) 1 μ M after hybridized with complementary DNA (dA ₉ , 1 μ M, blue) compared with single base mismatched DNA (dA ₅ TA ₄ , 1 μ M, red) in 10 mM phosphate buffer pH 7.0	102
Figure A24 Melting curves of PNAs MB-T9-Lys (top) T4-MB-T5 -Lys (bottom) 1 μ M after hybridized with complementary DNA (dA ₉ , 1 μ M, blue) compared with single base mismatch DNA (dA ₅ TA ₄ , 1 μ M, red) in 10 mM phosphate buffer pH 7.0	103
Figure A25 Melting curves of PNA 2AQ-WSSV-Lys (1 μ M) after hybridized with complementary DNA (1 μ M, blue) compared with three other single base mismatched DNA (1 μ M, red, green and purple) in 10 mM phosphate buffer pH 7.0.....	104
Figure A26 Melting curves of PNA 2AQ-WSSV-Lys (1 μ M) after hybridized with 19bp complementary (1 μ M) (top) and single base mismatched DNAs (1 μ M) (bottom) (blue: without NaCl, red: with 100 mM NaCl). The corresponding melting curves for DNA duplexes (dsDcomp19mer and dsDsmC19mer) (1 μ M) are shown in green (without NaCl) and purple (with 100 mM NaCl). All experiments were conducted in 10 mM phosphate buffer pH 7.0.....	105
Figure A27 Melting curves of PNAs 2AQ-B1502-Lys (top) and 2AQ-B1513-Lys (bottom) (1 μ M) after hybridized with complementary DNA (1 μ M, blue) and single base mismatched DNA (1 μ M, red) in 10 mM phosphate buffer pH 7.0	106
Figure A28 Melting curves of PNAs 2AQ-B1502-Lys (blue) and 2AQ-B1513-Lys (red) (top) (1 μ M each) after hybridized with 30bp complementary DNA targets (1 μ M) (top) and the melting curves for 30bp DNA duplexes corresponding to B1502 (1 μ M, blue) and B1513 (1 μ M, red) (bottom). All experiments were conducted in 10 mM phosphate buffer pH 7.0	107



LIST OF SCHEMES

	Page
Scheme 4.1 Working hypothesis of the present immobilization-free electrochemical DNA sensor.....	37
Scheme 4.2 Principle of immobilization-free DNA detection on the positively charged modified SPCE	43



LIST OF ABBREVIATIONS AND SYMBOLS

δ	Chemical shift (NMR)
A	Adenine
Abs	Absorbance
Acpc	(1 <i>S</i> ,2 <i>S</i>)-2-aminocyclopentanecarboxylic acid
Ac ₂ O	Acetic anhydride
Aeg	2-Aminoethyl glycine
Apc	3-Aminopyrrolidine-4-carboxylic acid
AQ	Anthraquinone
AQDS	Anthraquinone 2,6-disulfonic acid
Boc	<i>tert</i> -Butoxycarbonyl
bpy	2,2'-Bipyridine
Bz	Benzoyl
C	Cytosine
calcd	Calculated
CCA	α -cyano-4-hydroxy cinnamic acid
CDCl ₃	Deuterated chloroform
CHT	Chitosan
CV	Cyclic voltammetry
d	Doublet
DBU	1,8-Diazabicyclo[5.4.0]undec-7-ene
dd	Double of doublet
DIEA	Diisopropylethylamine
DM	Daunomycin
DMF	N,N'-dimethylformamide
dmp	Dimethyl-1,10-phenanthroline
DMSO- <i>d</i> ₆	Deuterated dimethylsulfoxide
DNA	Deoxyribonucleic acid
dNTPs	Deoxynucleotide triphosphates
DPV	Differential pulse voltammetry
ds	Double stranded
E	Potential
EDTA	ethylenediaminetetraacetic acid
equiv.	Equivalent



eT	Electron transfer
EtOAc	Ethyl acetate
Fc	Ferrocene
Fmoc	9-Fluorenylmethoxycarbonyl
G	Guanine
Glu	Glutamic acid
GPES	General Purpose Electrochemical System
HATU	<i>O</i> -(7-azabenzotriazol-1-yl)- <i>N,N,N',N'</i> -tetramethyluronium hexafluorophosphate
HCV	Hepatitis C virus
HLA	Human leukocyte antigen
HOAt	1-Hydroxy-7-azabenzotriazole
HPLC	High performance liquid chromatography
HPV	Human papiloma virus
HTACC	<i>N</i> -[(2-hydroxyl-3-trimethylammonium)propyl]chitosan chloride
Hz	Hertz
I	Current
Ibu	Isobutyryl
IHHNV	Infectious hypodermal and hematopoietic necrosis virus
ITO	Indium tin oxide
LAMP	Loop mediated isothermal amplification
LOD	Limit of detection
LOQ	Limit of quantitation
Lys	Lysine
M	Mega, Molar
m	Multiplet
MALDI-TOF	Matrix-assisted laser desorption/ionization-time of flight
MB	Methylene blue
MeCN	Acetonitrile
MeOH	Methanol
MES	2-Morpholinoethanesulfonic acid
MS	Mass spectrometry
mV	Millivolt
m/z	Mass to charge ratio
NMR	Nuclear magnetic resonance
Obs	Observed



OPfp	Pentafluorophenyl ester
PAA	Polyacrylic acid
PAH	Poly(allylamine) hydrochloride
PCR	Polymerase chain reaction
Pfp	Pentafluorophenyl
PfpOTfa	Pentafluorophenyl trifluoroacetate
phen	1,10-Phenanthroline
phi	Phenanthrenequinone diimine
PNA	Peptide nucleic acid
PQDMAEMA	Poly(quaternized dimethylamino)ethyl methacrylate
q	Quartet
R^2	Correlation coefficient
RNA	Ribonucleic acid
s	Singlet
ss	Single stranded
SER	Serine
SPCE	Screen-printed carbon paste electrode
SWV	Square-wave voltammetry
T	Thymine
^t Bu	tert-Butyl
Tfa	Trifluoroacetyl
TFA	Trifluoroacetic acid
TLC	Thin layer chromatography
T_m	Melting temperature
t_R	Retention time
Tris	Tris(hydroxymethane)aminomethane
TSV	Taura syndrome virus
UV	Ultraviolet
V	Volt
w/v	Weight per volume
WSSV	White Spot Syndrome Virus
YHV	Yellow-Head Virus

